Published in final edited form as:
Genes Brain Behav. 2008 July ; 7(5): 587–598. doi:10.1111/j.1601-183X.2008.00395.x.

Variation in *Galr1* expression determines susceptibility to excitotoxin-induced cell death in mice

S. Kong[†], **A. Lorenzana**[‡], **Q. Deng**[‡], **T. H. McNeill**[‡], and **P. E. Schauwecker**[*,‡]

[†]Department of Biochemistry and Molecular Biology, University of Southern California Keck School of Medicine, Los Angeles, CA, USA

[‡]Department of Cell and Neurobiology, University of Southern California Keck School of Medicine, Los Angeles, CA, USA

Abstract

Inbred strains of mice differ in their susceptibility to excitotoxin-induced cell death, but the genetic basis of individual variation in differential susceptibility is unknown. Previously, we identified a highly significant quantitative trait locus (QTL) on chromosome 18 that influenced susceptibility to kainic acid-induced cell death (*Sicd1*). Comparison of susceptibility to seizure-induced cell death between reciprocal congenic lines for *Sicd1* and parental background mice indicates that genes influencing this trait were captured in both strains. Two positional gene candidates, *Galr1* and *Mbp*, map to 55 cM, where the *Sicd1* QTL had been previously mapped. Thus, this study was undertaken to determine if *Galr1* and/or *Mbp* could be considered as candidate genes. Genomic sequence comparison of these two functional candidate genes from the C57BL/6J (resistant at *Sicd1*) and the FVB/NJ (susceptible at *Sicd1*) strains showed no single-nucleotide polymorphisms. However, expression studies confirmed that *Galr1* shows significant differential expression in the congenic and parental inbred strains. *Galr1* expression was downregulated in the hippocampus of C57BL/6J mice and FVB.B6-*Sicd1* congenic mice when compared with FVB/NJ or B6.FVB-*Sicd1* congenic mice. A survey of *Galr1* expression among other inbred strains showed a significant effect such that ‘susceptible’ strains showed a reduction in *Galr1* expression as compared with ‘resistant’ strains. In contrast, no differences in *Mbp* expression were observed. In summary, these results suggest that differential expression of *Galr1* may contribute to the differences in susceptibility to seizure-induced cell death between cell death-resistant and cell death-susceptible strains.

Keywords

Candidate genes; cell death; congenic mice; C57BL/6J; FVB/NJ; hippocampus; quantitative trait locus; seizure

Inbred mouse models offer an effective means of identifying candidate seizure-induced excitotoxic cell death susceptibility loci. Inbred strains of mice differ in their tendency to develop cell death after chemically induced seizure induction (McKhann *et al.* 2003; McLin & Steward 2006; Schauwecker 2003; Schauwecker & Steward 1997; Schauwecker *et al.* 2004; Shuttleworth & Connor 2001), but the genetic basis of variation in kainate-induced excitotoxicity is unknown. Genetic variation, through its effects on gene expression or function of the gene product, can determine individual phenotypic variation and disease susceptibility,

*Corresponding author: P. E. Schauwecker, Department of Cell and Neurobiology, University of Southern California Keck School of Medicine, 1333 San Pablo Street, BMT 403, Los Angeles, CA 90089-9112, USA. schauwec@usc.edu.

and, as a result, inbred mouse models have been used as the basis of genetic investigations to define susceptibility genes (Lorenzana *et al.* 2007; Schauwecker *et al.* 2004).

Linkage studies using (C57BL/6J × FVB/NJ)N2 mice mapped three susceptibility loci, with the most significant locus, named seizure-induced cell death 1 (*Sicd1*), to the distal region of mouse chromosome 18 (Schauwecker *et al.* 2004). To confirm genetic linkage on distal chromosome 18, we created the congenic strain, FVB.B6-*Sicd1*, in which the relevant donor segment from the resistant C57BL/6J strain was placed on the susceptible FVB/NJ background. The presence of C57BL/6 chromosome 18 alleles on an FVB genetic background conferred protection against seizure-induced cell death, as compared with FVB/NJ parental controls (Lorenzana *et al.* 2007; Schauwecker *et al.* 2004). These results suggested that the causal gene (s) influencing susceptibility to seizure-induced cell death may reside in the *Sicd1* locus.

As we verified that the *Sicd1* locus significantly reduced susceptibility to kainic acid (KA)-induced excitotoxic cell death in the congenic FVB.B6-*Sicd1* strain (Lorenzana *et al.* 2007; Schauwecker *et al.* 2004), we took a candidate gene approach to identify the causal susceptibility gene(s) responsible for the *Sicd1* effect. The genetic variation underlying this quantitative trait locus (QTL) could consist of polymorphisms in either the coding region, thus altering the amino acid sequence of the translated protein, or the regulatory region, affecting expression of a gene. Among the many candidate genes present in the 12-Mb *Sicd1* region, galanin receptor 1 (*Galr1*) and *myelin basic protein* (*Mbp*) are the most compelling. Both of these genes approximate the peak position of the *Sicd1* QTL at 55 cM (Schauwecker *et al.* 2004) and have relevance to modulation of neuronal excitability and seizure threshold (Donarum *et al.* 2006; Jacoby *et al.* 2002; Mathis *et al.* 2000; Mazarati *et al.* 2000, 2006; McColl *et al.* 2006; Zini *et al.* 1993b).

In this paper, we describe a systematic gene identification strategy in which we conducted comparative genomic sequencing, expression analyses and comparative cDNA sequencing of two putative candidate genes, *Galr1* and *Mbp*. To examine the possibility that variation in one of these genes could be involved in the susceptibility to seizure-induced excitotoxic cell death, we assessed the expression of mRNA for *Galr1* and *Mbp* in the hippocampus of our two strains and between the FVB.B6-*Sicd1* and the B6.FVB-*Sicd1* congenic strains and their respective parental background strains, FVB/NJ or C57BL/6J. We also conducted a strain survey to examine the association between the *Sicd1* genotype and the susceptibility to seizure-induced cell death among inbred strains of mice.

Materials and methods

Mice and generation of the congenic FVB.B6-Sicd1 and B6.FVB-Sicd1 strains

Male C57BL/6J, FVB/NJ, BALB/cJ, DBA/2J, SJL/J and 129T2/SvEmsJ mice were purchased from the Jackson Laboratory (Bar Harbor, ME, USA) at age 6–8 weeks. The congenic FVB.B6-*Sicd1* and B6.FVB-*Sicd1* strains were generated at the Zilkha Neurogenetic Institute at the University of Southern California Keck School of Medicine, as previously described (Schauwecker *et al.* 2004). All mice were maintained on a 12-h light/dark schedule with food and water available *ad libitum*. All experiments were approved by the University of Southern California Institutional Animal Care and Use Committee, in accordance with The National Institutes of Health *Guide for the Care and Use of Laboratory Animals*.

Quantitative polymerase chain reaction

For RNA isolation, mice were anesthetized with Avertin and killed by decapitation. Whole brains were removed by dissection and both hippocampi were rapidly dissected out on ice. Both combined hippocampi from a mouse whole brain (~50 mg) were homogenized and total

RNA was extracted using the RiboPure kit™ (Ambion, Austin, TX, USA) following manufacturer's protocols. The quantity and quality of RNA were estimated with spectrophotometric analysis ($OD_{260/280}$) and RNA was stored at −20°C. Reactions were set up for two-step reverse transcriptase polymerase chain reaction (RT-PCR).

First-strand cDNA was synthesized from total hippocampal RNA with random decamers using Reverse-IT RTase Blend™ (Abgene, Rochester, NY, USA). Relative basal hippocampal transcript levels were measured using the SYBR Green real-time quantitative PCR method following manufacturers' instructions (Applied Biosystems, Foster City, CA, USA; Roche Applied Sciences, Indianopolis, IN, USA). Primer sequences for *Galr1*, *Mb*p and β-actin were designed using primer 3 (Rozen & Skaletsky 2000; summarized in Table 1) based on the murine *Galr1, Mbp* and β-actin sequences obtained from the Ensembl genome browser (release 36). All primers were purchased from Sigma-Genosys (The Woodlands, TX, USA) as high-performance liquid chromatography purified oligos and were tested to determine whether they produced a single band on an agarose gel. At least two independent replicate experiments were performed for each gene, and all samples were run in triplicate to minimize intra-assay variation. Primers were further evaluated by melting curve analysis of the PCR product to check amplification of a single major peak at a temperature compatible with the amplicon size and base composition.

For very discrete expression changes, we used the relative standard curve method, which gives highly accurate quantitative results and requires the least amount of validation (Applied Biosystems). Standard curves were prepared for the target (*Galr1* or *Mbp*), and the endogenous control, β-actin, and the quantity of the target was normalized to the quantity of β-actin. β-actin was used as an internal reference gene because it had smaller variability among individual mouse strains than other housekeeping genes, such as glyceraldehyde 3-phosphate dehydrogenase or 18s rRNA. The same pool of standard cDNA was used for generation of standard curves throughout the study to ensure the accuracy of real-time PCR results.

The ratio of target gene mRNA expression for each individual strain as compared with C57BL/6J mice was determined according to the standard curve method. This method determines the changes in the target gene expression relative to changes in the internal standard (β-actin) and corrects for differences in the efficiency of amplification for the primer pairs for each gene. Statistical significance was determined using a one-way analysis of variance (ANOVA) and intergroup differences were analyzed by a Student Newman–Keuls post hoc analysis using the statistical software package, SIGMASTAT 3.0 (Jandel Scientific, San Rafael, CA, USA). Data are presented as the mean ± SEM, and were considered significant at $P < 0.05$.

Galr1 and *Mbp* genomic sequencing

The *Galr1* gene has three coding exons spanning 13.3 kb of genomic DNA and gives rise to a 348-amino-acid protein. The *Mbp* gene has seven coding exons spanning 110.5 kb of genomic DNA and gives rise to a 250-amino-acid protein. *Galr1* and *Mbp are* arranged in a divergent direction separated by 68 kb of genomic sequence on mouse chromosome 18qE, 55 cM. The genomic DNA sequence of the promoter, 5′-untranslated region (UTR), all coding exons, 3′-UTR and splice sites on *Galr1* and *Mbp* was determined in a total of two C57BL/6J and six FVB/NJ mice by PCR amplification of genomic DNA. Briefly, a small piece (~1 cm) of the tip of the tail of each of the C57BL/6J and FVB/NJ mice was cut off using sharp scissors. Mouse tail genomic DNA was extracted and purified using the DNeasy kit™ (Qiagen, Valencia, CA, USA) following manufacturers' protocols.

Sequencing primers for *Galr1* and *Mbp* were designed using primer 3 (Rozen & Skaletsky 2000; Tables 2 and 3) based on the murine *Galr1* and *Mbp* sequences obtained from the Ensembl genome browser (release 36). All primers were purchased from Sigma-Genosys) as

unpurified desalted oligos. Mouse tail genomic DNA was amplified with gene-specific primers by standard 50-μl PCR reactions (Dieffenbach *et al.* 1993). Amplification conditions included 35 cycles of denaturation at 94°C for 30 seconds, annealing at the optimal temperature of each primer pair for 30 seconds and extension at 72°C for 50 seconds with initial denaturation at 94°C for 3 min and final extension at 72°C for 3 min. The resulting PCR products were resolved on 2% ethidium bromide-stained agarose gels and the purity of amplified PCR fragments was verified as a single sharp band. Bands of appropriate size were excised with a razor blade, purified and extracted using QIAEX II Gel Purification kits™ (Qiagen) according to manufacturers' instructions.

Both *Galr1* strands of each amplicon were sequenced using the corresponding forward and reverse PCR primers and 806 bp of the Galr1 promoter region was sequenced using a TOPO TA cloning kit for sequencing (Invitrogen) following manufacturers' instructions. The 806-bp amplicon was gel purified and subcloned into pCR 4-TOPO (Invitrogen) before sequencing. DNA sequencing was performed by the Norris Cancer Facility at University of Southern California (USC) on an Applied Biosystems 3730 DNA analyzer by the Big Dye Terminator Cycle Sequencing kit, version 3 (Perkin-Elmer Biosystems, Foster City, CA, USA). Sequencing results were manually checked to eliminate any possible miss-calls and then analyzed using T-Coffee version 2.00 (Notredame *et al.* 2000) to align DNA sequences between the C57BL/6J and the FVB/NJ mouse strains.

Hippocampal *Galr1* cDNA sequencing

The cDNA prepared from hippocampal RNA of 6- to 8-week-old male C57BL/6J and FVB/NJ mice was used for mutation screening. The primer pair amplifying the 1904-bp full-length *Galr1* transcript was designed using primer 3 (Rozen & Skaletsky 2000; summarized in Table 4) based on the murine *Galr1* sequence obtained from the Ensembl genome browser (release 36). Standard 50-μl PCR reactions (Dieffenbach *et al.* 1993) were performed on 10 μl of first-strand hippocampal cDNA synthesis reaction using the primer pair amplifying the 1904-bp full-length hippocampal *Galr1* transcript. Amplification conditions included 40 cycles of denaturation at 94°C for 45 seconds, annealing at 57°C for 45 seconds and extension at 68°C for 2 min 30 seconds, with initial denaturation at 94°C for 3 min and final extension at 68°C for 15 min.

The purity of amplified PCR fragments was verified as a single sharp band on an ethidium bromide-stained agarose gel. Bands of 1904 bp were excised with a razor blade, purified and extracted using the QIAEX II™ gel purification kit (Qiagen) according to manufacturers' instructions. The resulting 1904-bp amplicon was subject to direct sequencing using primers summarized in Table 5 to detect any potential aberrant splicing and/or any potential amino acid polymorphism(s). Complementary DNA sequencing was performed on an ABI 3730 DNA analyzer by cycle sequencing using 3′-fluorescent-labeled dideoxynucleotides (dye terminator chemistry). All chromatogram data were checked manually to eliminate any possible miss-calls and sequencing results were analyzed using T-Coffee (Notredame *et al.* 2000) to align DNA sequences between the two mouse strains.

Kainic acid administration

Adult male C57BL/6J, FVB/NJ, BALB/cJ, DBA/2J, SJL/J and 129T2/SvEmsJ, homozygous FVB.B6-*Sicd*1 and homozygous B6.FVB-*Sicd*1 congenic mice (6–8 weeks old) were used in these studies. Kainic acid (Diagnostic Chemical, Ltd, Charlottetown, PEI, Canada) was dissolved in isotonic saline (pH 7.3) and administered s.c. to adult male mice. Preliminary dose response studies had defined seizure thresholds and showed consistent seizures among all six inbred mouse strains and both congenic strains, with a mortality of less than 25% with a dose of 25 mg/kg, s.c. (Schauwecker & Steward 1997). Kainic acid solutions were prepared fresh

on the day of each experiment. Following KA injections, mice were monitored every 15 min for 4 h to determine seizure parameters: the onset, the duration and percentage of mice achieving each seizure stage according to the Racine classification of seizure stages (Racine 1972).

Histological staining

In order to evaluate the severity of KA-induced excitotoxic brain damage in different strains of mice, brains from each strain of mice were processed for light microscopic histopathologic evaluation according to previously published methods (Schauwecker *et al.* 2004). Briefly, 7 days after seizure induction by KA, mice were anesthetized with Avertin and transcardially perfused with 4% paraformaldehyde in 0.1 M phosphate buffer (pH 7.4). Brains were removed and post-fixed in 30% sucrose for at least 12–18 h for cryoprotection. Horizontal (35 μm) sections were cut on a sliding microtome and immersed in phosphate buffer (pH 7.4); free floating until histological processing was started. Every sixth section (~210 μm) was processed for cresyl violet staining to assess cell loss and morphology. An alternate series of sections were stained with a modified Gallyas silver stain, which stains degenerating fibers, synaptic terminals and cell bodies (Nadler & Evenson 1983 as modified in Schauwecker 2003) and examined for the appearance of degenerative debris. An additional series of sections were stained with Fluoro-Jade B, a fluorescent marker for dying neurons, according to the method outlined previously (Schmued & Hopkins 2000).

Morphological assessment of neuronal damage

The number of degenerating neurons in both the right and the left hippocampus from every sixth section (240-μm separation distance) in four brain regions (CA3, CA1, dentate hilus and dentate gyrus), which represented various levels of the hippocampus, was visually estimated and a histological damage score was assigned on a 0–3 grading scale according to the following criteria: grade 0, absence of pyknotic cells; grade 1.0, mild (<25% of cells pyknotic); grade 2.0, moderate (<50% of hippocampal neurons pyknotic) and grade 3.0, extensive (>50% of cells pyknotic) according to a previously defined scale (Fujikawa 1995, 1996; Fujikawa *et al.* 1994; Schauwecker *et al.* 2004). All grading was performed blindly by an observer who was naïve to the strain.

There was no obvious difference in neuronal damage between hemispheres, so values for right and left hemispheres were averaged for each mouse. For the hippocampus, scores from sections were averaged and used for calculating group values. As histological damage scores were normally distributed, we were able to use standard parametric methods of data analysis. Thus, to determine whether differences in histological scores existed among the groups of mice, results were assessed statistically by one-way ANOVA with the computer program SIGMASTAT version 3.00 (Jandel Scientific) and intergroup differences were analyzed by Student Newman–Keuls post hoc test.

Neuronal loss quantification

We counted cells in defined areas of CA1, CA3, the dentate hilus and the dentate gyrus in a blinded manner using unbiased stereological methods on cresyl violet-stained sections as described (Schauwecker & Steward 1997; Schauwecker *et al.* 2000). The Nissl-stained neurons in area CA3, area CA1, the dentate hilus and the dentate gyrus were counted in both the right and the left hippocampus and counting was initiated within the ventral hippocampus at the first point where hippocampal subfields could be easily identified. This level corresponded to horizontal section 54, based on the atlas of Sidman *et al.* (1971). Hippocampal subfields were based on Franklin and Paxinos (1997) classification and discrimination between the CA3 and the dentate hilus region was based on morphological features and locations of the cells (Sousa *et al.* 1998; West *et al.* 1991). Specifically, for dentate hilar cell counts, the hilus was

operationally defined as the region bordered by the supra- and infrapyramidal granule cell layers and excluding the densely packed pyramidal neurons of area CA3.

Neuron counts were made in all subfields and the numbers for each side were averaged into single values for each animal. Surviving cells were counted only if they were contained within the pyramidal cell layer, dentate hilus or dentate gyrus, possessed a visible nucleus and characteristic neuronal morphology and had a cell body larger than 10 μm. Six square counting frames (200 × 200 μm) were randomly placed in the pyramidal layer of fields CA1 and CA3 or in the dentate hilus or dentate gyrus in 4–5 regularly spaced horizontal sections from each animal. Neuronal nuclei were evaluated at three different focal planes and only those in the focal plane were counted with a × 40 objective and considered as a counting unit. Stereological analysis was performed with the aid of IMAGE-PRO PLUS software version 4.00 (Media Cybernetics, Inc., Silver Spring, MD, USA) in combination with a SPOT digital camera (Diagnostic Instruments, Inc., Sterling Heights, MI, USA) and a motorized Z-stage (Optiscan, Prior Scientific, Fairfax, VA, USA). Final cell counts are expressed as the percentage of cells as compared with intact mice. Results were assessed statistically by one-way ANOVA using the computer program, SIGMASTAT version 3.00 (Jandel Scientific), and intergroup differences were analyzed by the Student Newman–Keuls post hoc test. Data were considered significant at $P < 0.05$.

Results

Phenotypic analysis of susceptibility to seizure-induced cell death in Sicd reciprocal congenic strains

In order to further confirm the chromosome 18 QTL, termed *Sicd1*, reciprocal congenic lines were constructed for the *Sicd1* interval (D18Mit141–D18Mit25). For FVB.B6-*Sicd1* congenic mice, we introgressed the interval containing the putative resistant B6 alleles onto the susceptible FVB background. In contrast, for the B6.FVB-*Sicd1* congenic mice, we introgressed the interval containing the putative susceptibility FVB alleles onto the resistant B6 background. Phenotypic analysis of the extent of seizure-induced cell death in both strains confirmed that a gene(s), located between the D18Mit141 and the telomere on chromosome 18, plays an intrinsic role in susceptibility to seizure-induced cell death. This conclusion is supported by data showing the dramatic reduction in susceptibility to seizure-induced cell death with the FVB.B6-*Sicd1* strain relative to the FVB background strain (Fig. 1; Lorenzana *et al.* 2007), and the significant increase in susceptibility to seizure-induced cell death within the B6.FVB-*Sicd1* strain relative to the B6 background strain (Fig. 1).

Prioritization of candidate genes

As we were able to verify that the *Sicd1* QTL significantly affected susceptibility to seizure-induced cell death in our congenic FVB.B6-*Sicd1* strain (Schauwecker *et al.* 2004), we sought to identify candidate genes within the *Sicd1* interval (D18Mit141–D18Mit25) that might explain this effect. The peak LOD (D18Mit186–D18Mit4) of *Sicd1* covers about 13 Mb (the physical interval 72–85 Mb). However, the region defined by a one LOD drop (the 99% confidence interval for the true QTL location) is about 5 Mb (the physical interval 79–84 Mb) (Schauwecker *et al.* 2004). Analysis of the *Sicd1* gene content indicates that this reduced 5-Mb region contains approximately 12 genes that show homology with the human genome (The Build 36 assembly by National Center for Biotechnology Information (NCBI); Fig. 2). Among the 12 genes within this region, we identified two potential *Sicd1*-encoded candidate genes, *Galr1* and *Mbp*, based on the following criteria: (1) physically residing in the *Sicd1* locus, (2) detected as expressed in the hippocampus as shown in the Allen Brain Atlas (http://www.brain-map.org/aba/mouse/brain/Galr1.html;

http://www.brain-map.org/aba/mouse/brain/Mbp.html), (3) human homology and (4) correlated with hippocampal excitability and/or hyperexcitability.

Galr1 mRNA is differentially expressed in congenic and background strains

We hypothesized that strain-specific genetic variation, through its effects on gene expression, in one or more genes between C57BL/6J (B6) and FVB/NJ (FVB) is responsible for the *Sicd1* effect. To investigate further whether variation in *Galr1* expression determines susceptibility to KA-induced excitotoxic cell death, we measured the basal hippocampal transcript abundances of *Galr1* to determine if variation in *Galr1* expression is associated with susceptibility to KA-induced excitotoxic cell death. We used quantitative real-time PCR (qRT-PCR) because *Galr1* is expressed at a relatively low level in the hippocampus. We found a significant difference in basal levels of *Galr1* transcripts that were ~40% less in a cell death-resistant B6 than in a cell death-susceptible FVB hippocampi (Fig. 3a).

Similarly, in homozygous FVB.B6-*Sicd1* congenic and parental background FVB mice, quantitative PCR verified the strain-specific pattern of *Galr1* gene expression with respect to the B6 congenic segment. Specifically, *Galr1* mRNA expression was downregulated (~45%) in congenic hippocampus as compared with FVB (Fig. 3b). In contrast, quantitative PCR verified that *Galr1* mRNA expression was significantly increased in the hippocampus of B6.FVB-*Sicd1* congenic mice as compared with C57BL/6J mice. A clear relationship was found: congenic FVB.B6-*Sicd1* with the B6 allele at *Galr1* showed significantly lower levels of hippocampal *Galr1* expression than control FVB littermates, whereas congenic B6.FVB-*Sicd1* with the FVB allele at *Galr1* showed significantly higher levels of hippocampal *Galr1* expression than control B6 littermates.

Inbred strains are differentially susceptible to KA-induced excitotoxic cell death

We previously found that certain inbred mouse strains show marked differences in susceptibility to KA-induced excitotoxic cell death (Schauwecker & Steward 1997). In the present study, we assessed two additional strains, SJL/J and DBA/2J for susceptibility to KA-induced excitotoxic cell death. Preliminary dose response studies defined seizure thresholds and showed consistent seizures among all six inbred mouse strains, with a mortality of less than 25% when a dose of 25 mg/kg was administered s.c. (Schauwecker & Steward 1997). Systemic administration of KA induced a characteristic sequential behavioral response: stage 1, immobility; stage 2, forelimb and/or tail extension, rigid posture; stage 3, repetitive movements, head bobbing; stage 4, rearing and falling; stage 5, continuous rearing and falling; stage 6, severe tonic-clonic seizures. Table 5 summarizes the percentage of animals achieving each seizure stage (1–5) and the duration of severe seizures for all six strains. Severe seizures (stages 4 and 5) lasted on average 1.6 h and no significant strain-dependent effects were found with regard to qualitative differences in seizure intensity or the percentage of animals achieving stage 5 seizures among the representative strains. However, a significant strain-dependent difference in the duration of stage 5 seizures was observed in DBA/2J (cell death-susceptible) and in SJL/J (cell death-resistant) strains as compared with the other strains.

We assessed KA-induced excitotoxic neuronal death in the six strains of mice by light microscopic histopathologic evaluation. Systemic administration of KA induced the degeneration and reduction of hippocampal neurons in area CA3, the dentate hilus and sporadic neuronal reduction in area CA1 in susceptible strains (Fig. 3c–e; FVB/N, DBA/2J and 129T2/SvEmsJ). Consistent with previous studies (Ben-Ari *et al.* 1984; Nadler & Cuthbertson 1980; Nadler *et al.* 1980; Sperk *et al.* 1983), neurons within the dentate granule cell layer and area CA2 were spared. In contrast, three representative resistant strains (C57BL/6J, BALB/cJ and SJL/J) showed no detectable reduction of neurons within the hippocampus proper and no indication was noted of damage to neuronal nuclei in any hippocampal region or in the septum,

amygdala, pyriform cortex, neocortex or thalamic nuclei in cresyl violet-stained sections (Fig. 4). In addition, sections from susceptible mice that were processed for the Gallyas silver stain for degeneration displayed intense argyrophilic deposits within the stratum oriens and stratum pyramidale of the CA3 subfield and within the dentate hilus. In contrast, those strains resistant to excitotoxic cell death displayed no detectable evidence of degenerative debris or reduction of neurons in any of the hippocampal subfields after KA administration.

To confirm these results, we performed quantitative analyses of hippocampal neuron numbers. The susceptible strains (FVB/NJ, DBA/2J and 129T2/SvEmsJ) showed a reduction on average of 43% of dentate hilar neurons, 70% of CA3 pyramidal neurons and 38% of CA1 pyramidal neurons 7 days after KA administration as compared with wild-type control injected with the same amount of saline ($F(1,5) = 66.413$; $P < 0.001$; Fig. 5). These results indicated that KA induces differential vulnerability of neurons in the hippocampus in a strain-dependent manner although KA-induced seizures are qualitatively comparable.

Haplotype analysis of hippocampal *Galr1* mRNA expression

To confirm the hypothesis that differences in susceptibility to seizure-induced cell death are associated with variation in the expression of *Galr1*, we conducted haplotype analyses on a total of six inbred mouse strains, divergent for the phenotype of seizure-induced cell death to determine whether variation in *Galr1* expression observed among FVB and B6 strains was conserved as a whole in other inbred mouse strains. Quite clearly, we found that the representative cell death-resistant strains (C57BL/6J, BALB/cJ and SJL/J) showed significantly lower hippocampal *Galr1* expression levels than did representative cell death-susceptible strains (FVB/NJ, DBA/2J and 129T2/SvEmsJ) (Fig. 6). Thus, we confirmed and extended the results observed among FVB and B6 strains.

Sequencing and identification of single-nucleotide polymorphisms in *Galr1*

As the *Galr1* locus may be associated with susceptibility to KA-induced excitotoxic cell death in mice, we searched for underlying sequence variation of the *Galr1* gene between B6 and FVB strains. To look for variation that could predict a functional consequence, the coding region of *Galr1* was sequenced from the B6 and FVB inbred strains. We found no sequence differences in the coding region of *Galr1*. Similarly, no identified sequence alterations were found between the FVB and the B6 inbred strains within any of the 5′- or 3′-regulatory regions, splice sites or promoter region (Fig. 7).

Hippocampal *Mbp* mRNA expression and sequence analyses

Mbp is widely distributed in a number of tissues, but available data show some of the highest expression in brain (Mathisen *et al.* 1993). Using quantitative PCR, we found that *Mbp* was not differentially regulated in the hippocampus of either FVB or B6 or homozygous FVB.B6-*Sicd1* congenic mice (Fig. 8a,b). Although we found no significant strain-dependent difference in basal expression for *Mbp*, genetic variation can affect the function of the gene product, and we searched for sequence variation of the *Mbp* gene between B6 and FVB strains as well. We manually sequenced the promoter, 5′-UTR, all seven coding exons, 3′-UTR, and splice sites of *Mbp* on B6 and FVB genomes. Similar to our results for *Galr1*, we found no sequence variation in the promoter, 5′-UTR, all coding exons, 3′-UTR and splice sites for *Mbp* (Fig. 9).

The cDNA sequence analysis of *Galr1*

Any critical DNA sequence change(s) underlying *Sicd1* could be a result of changes in the protein-coding region that change the encoded protein or of changes in the regulatory region of the gene that influence expression of the gene. Here, we sequenced the protein-coding region of *Galr1* using the B6 and FVB progenitor strains to detect any potential amino acid

polymorphism(s) caused by nuclear post-transcriptional RNA editing (Fig. 10). We PCR amplified the whole 1904-bp amplicon of full-length *Galr1* cDNA and subsequently subjected it to sequencing in C57BL/6J and FVB/NJ strains. No variation in cDNA sequence was observed between the two inbred strains examined.

Discussion

Phenotyping studies of a new congenic strain developed in our laboratory have confirmed the significant genetic influence of a chromosome 18 QTL: *Sicd1* for susceptibility to seizure-induced cell death (Schauwecker *et al.* 2004). To validate the *Sicd1* effect and to move towards identification of the quantitative trait gene(s) for *Sicd1*, we generated reciprocal congenic lines of mice. These strains were differentially susceptible to seizure-induced cell death because they had received a chromosomal donor region from either FVB/NJ that contained the susceptible *Sicd1* alleles (B6.FVB-*Sicd1*) or C57BL/6J that contained the resistant *Sicd1* alleles (FVB.B6-*Sicd1*). These results give additional support for *Sicd1* containing a gene (or a set of closely linked genes) contributing to seizure-induced cell death.

Because these congenic strains retained the phenotype of the original linked QTL, we hypothesized that candidate genes responsible for conferring susceptibility to seizure-induced excitotoxic cell death were present within the identified 12-Mb *Sicd1* interval on chromosome 18. The mechanism(s) underlying phenotypic strain differences in susceptibility to seizure-induced cell death could involve genes affecting hippocampal excitability, hyperexcitability and glutamate release. Therefore, genes encoding proteins involved in these processes are likely candidates for modifying susceptibility to KA-induced excitotoxic cell death. Two such genes in the reduced *Sicd1* interval satisfied this functional criteria, *Galr1* and *Mbp,* and were subjected to candidate gene analysis. Combining the gene expression data generated in the congenic FVB.B6-*Sicd1* strain with the association data of inbred strains of mice segregating for the trait of susceptibility to KA-induced excitotoxic cell death, we were able to identify *Galr1* as a putative causal susceptibility gene for KA-induced excitotoxicity. In contrast, we did not find any evidence to support *Mbp* as a causal susceptibility gene for KA-induced excitotoxicity.

It was hypothesized that the gene(s) producing the difference in response to kainate-induced cell death between B6 and FVB mice would be differentially expressed in the hippocampus of untreated control mice. We were especially interested in the *Galr1* and *Mbp* candidate genes because of their published associations with modifying hippocampal excitability and modifying hyperexcitability (Ben-Ari 1990; Donarum *et al.* 2006; Mazarati *et al.* 2000; Noveroske *et al.* 2005). To confirm the identity of any putative candidate genes, expression studies were performed using qRT-PCR, and any gene expression differences observed would presumably be the result of changes in allele frequencies because of selection rather than a response to kainate treatment. We found that B6 mice showed reduced levels of hippocampal *Galr1* mRNA as compared with FVB mice. Second, the congenic FVB.B6-*Sicd1* strain carrying the B6-derived resistant allele at the *Sicd1* region, where *Galr1* is located, on the FVB genetic background showed significantly decreased basal hippocampal *Galr1* expression compared with the susceptible FVB control littermates. In contrast, the congenic B6.FVB-*Sicd1* strain carrying the FVB-derived susceptible allele at the *Sicd1* region on the B6 genetic background showed significantly enhanced basal hippocampal *Galr1* expression compared with the resistant B6 control littermates.

We speculate that the downregulation of *Galr1* observed in B6 and FVB.B6-*Sicd1* mice supports its role as a modulator of neuronal excitability in the hippocampus (Ben-Ari 1990; Zini *et al.* 1993a,b). This speculation is supported by two lines of evidence suggesting that the neuropeptide galanin is a powerful regulator of seizure activity and neuronal excitability.

Previous studies have showed that acute administration of galanin receptor agonists can effectively attenuate convulsive activity induced by the pro-convulsant picrotoxin (Mazarati & Lu 2005) and can delay kindling epileptogenesis (Mazarati *et al.* 2006). Second, loss-of-function experiments have showed enhanced susceptibility to excitotoxin-induced neuronal injury in Galr1 knockout mice (Mazarati *et al.* 2004), and a recent study by McColl *et al.* (2006) show Galr1 knockout mice exhibit spontaneous partial seizures with impaired synaptic inhibition in the hippocampus. In contrast, gain-of-function experiments have showed that galanin overexpression is known to decrease hippocampal neuronal injury resulting from limbic seizures (Haberman *et al.* 2003; Mazarati *et al.* 2000) presumably through Galr1 receptor modulation (Mazarati & Lu 2005). Furthermore, the fact that our reciprocal congenic strains were differentially susceptible to seizure-induced cell death would suggest that differences in the level of *Galr1* expression alone may be sufficient to confer enhanced susceptibility to KA-induced neuronal death on a genetically resistant background, as was the case for the B6.FVB-*Sicd1* congenic strain. Thus, taken together, our findings support the observation that Galr1 can regulate neuronal excitability in the hippocampus.

We predicted that the gene, or regulatory region of the gene, producing the difference in response to kainate between B6 and FVB mice would be polymorphic between these two strains. Thus, we documented the sequence variation between these strains for the putative candidate genes, *Galr1* and *Mbp*. Sequence analysis showed no sequence variation in the promoter, 5′ -UTR, coding exons, 3′-UTR or splice sites for *Galr1* or *Mbp* between B6 and FVB strains. While sequence analysis of *Galr1* detected no polymorphisms in the regions analyzed, it is important to note that SNPs in noncoding sequences may also affect the levels and forms of mRNA transcripts. However, based on a survey of SNPs identified in the Perlegan mouse database (http://mouse.perlegen.com/mouse/) in conjunction with the Center for Rodent genetics (http://www.niehs.nih.gov/crg/) and for intronic regions of *Galr1* and *Mbp*, there is no evidence that an SNP in a noncoding region exists between FVB and B6. Second, while sequence analysis of *Galr1* detected no polymorphisms, we cannot rule out *Galr1* as a putative QTL gene. For example, *Galr1* could be differentially regulated by an upstream mechanism. The downregulation of *Galr1* expression in the hippocampus of B6 and FVB.B6-*Sicd1* mice indicates a positive association between *Galr1* expression and reduced susceptibility to excitatory amino acid-induced cell death. Whether or not changes in *Galr1* activity are involved in producing the phenotype of reduced susceptibility remains to be determined. The mechanism by which *Galr1* could influence susceptibility in this mouse model is not yet known, but could result from changes in the regulatory region of the gene, as suggested by the observed strain differences in expression.

While we did not find any evidence to support *Mbp* as a causal susceptibility gene for KA-induced excitotoxicity, there is still a possibility that other gene(s) within the *Sicd1* region are involved as well. Of the 12 known genes in the region defined by the one LOD drop (79–84 Mb), five of these have been published on. For example, a nucleotide substitution in the gene encoding *Ctdp1* results in an autosomal recessive disorder called congenital cataracts facial dysmorphism neuropathy (Varon *et al.* 2003). *Nfatc1* is considered as the master transcription factor for osteoclasts – the bone resorbing cells that play a key role both in the normal bone remodeling and in the skeletal osteopenia of arthritis, osteoporosis, periodontal disease and certain malignancies (Sato *et al.* 2007; Zhao *et al.* 2007). *Sall3* is a member of the Spalt gene family that encodes putative transcription factors. These Spalt homologues are widely expressed in neural and mesodermal tissues during early embryogenesis. *Sall3* is required for the development of nerves that are derived from the hindbrain and for the formation of adjacent branchial arch derivatives (Parrish *et al.* 2004) and has also been showed to be an epigenetic hotspot of aberrant DNA methylation (Ohgane *et al.* 2004). *Setbp1* is a protein that binds to the acute undifferentiated leukemia-associated protein, SET. SET is thought to play a key role in leukemogenesis by its nuclear localization and protein–protein interactions. While the

function of *Setbp1* remains unknown, it has been proposed to play a key role in the mechanism of SET-related leukemogenesis and tumorigenesis (Minakuchi *et al.* 2001). Lastly, *Pard6g* (Par6) is a key member of a multicomponent polarity complex that controls a variety of cellular processes, such as asymmetric cell division, establishment of epithelial apico-basal polarity and polarized cell migration (Bose & Wrana 2006; Yoshimura *et al.* 2006). While none of these genes, at present, is thought to play a relevant role in modulating neuronal excitability on its own, we cannot exclude that some of these genes, which play important roles in cellular-signaling pathways might be involved subsequently at some level. However, at present, we can only provide evidence that *Galr1* is at least one of the causal susceptibility genes for KA-induced excitotoxic cell death in mice.

In summary, our results identify *Galr1* as a promising candidate gene, but additional work is necessary to establish with certainty that *Galr1* is a seizure-induced cell death susceptibility gene. Until then, it must be kept in mind that another gene within the QTL interval in linkage disequilibrium with *Galr1* may ultimately be shown to contribute all or part of the QTL effect. Importantly, our congenic model and prospective sublines will be used to narrow and refine the differential locus on chromosome 18, as well as to examine gene interactions and subphenotypes in the control of excitatory amino acid-induced cell death susceptibility, with the ultimate goal of identifying the set of genes responsible for this complex trait. Validation of *Galr1* as causal for the trait of susceptibility to seizure-induced cell death will involve the construction of animals that are genetically altered with respect to *Galr1* activity followed by screens for variations in the trait of susceptibility to seizure-induced cell death.

Acknowledgments

This work was supported by NIH NS38696 to Paula Elyse Schauwecker. We thank Dr Wayne Frankel and Dr Thomas McCown for thoughtful comments on the manuscript and helpful discussions.

References

Ben-Ari Y. Galanin and glibenclamide modulate the anoxic release of glutamate in rat CA3 hippocampal neurons. Eur J Neurosci 1990;2:62–68. [PubMed: 12106103]

Ben-Ari Y, Tremblay E, Berger M, Nitecka L. Kainic acid seizure syndrome and binding sites in developing rats. Brain Res 1984;316:284–288. [PubMed: 6467019]

Bose R, Wrana JL. Regulation of Par6 by extracellular signals. Curr Opin Cell Biol 2006;18:206–212. [PubMed: 16490351]

Dieffenbach CW, Lowe TM, Dveksler GS. General concepts for PCR primer design. PCR Methods Appl 1993;3:S30–37. [PubMed: 8118394]

Donarum EA, Stephan DA, Larkin K, Murphy EJ, Gupta M, Senepharnsiri H, Switzer RC, Pearl PL, Snead OC, Jakobs C, Gibson KM. Expression profiling reveals multiple myelin alterations in murine succinate semialdehyde dehydrogenase deficiency. J Inherit Metab Dis 2006;29:143–156. [PubMed: 16601881]

Franklin, KBJ.; Paxinos, G. The Mouse Brain in Stereotaxic Coordinates. Academic Press; New York: 1997.

Fujikawa DG. Neuroprotective effect of ketamine administered after status epilepticus onset. Epilepsia 1995;36:186–195. [PubMed: 7821277]

Fujikawa DG. The temporal evolution of neuronal damage from pilocarpine-induced status epilepticus. Brain Res 1996;725:11–12. [PubMed: 8828581]

Fujikawa DG, Daniels AH, Kim JS. The competitive NMDA receptor antagonist CGP 40116 protects against status epilepticus-induced neuronal damage. Epilepsy Res 1994;17:207–219. [PubMed: 7912191]

Haberman RP, Samulski RJ, McCown TJ. Attenuation of seizures and neuronal death by adeno-associated virus vector galanin expression. Nat Med 2003;9:1076–1080. [PubMed: 12858168]

Jacoby AS, Hort YJ, Constantinescu G, Shine J, Iismaa TP. Critical role for GALR1 galanin receptor in galanin regulation of neuroendocrine function and seizure activity. Mol Brain Res 2002;107:195–200. [PubMed: 12487125]

Lorenzana A, Chancer Z, Schauwecker PE. A QTL on chromosome 18 is a critical determinant of excitotoxic cell death susceptibility. Eur J Neurosci 2007;25:1998–2008. [PubMed: 17439488]

Mathis C, Hindelang C, LeMeur M, Borrelli E. A transgenic mouse model for inducible and reversible dysmyelination. J Neurosci 2000;20:7698–7705. [PubMed: 11027231]

Mathisen PM, Pease S, Garvey J, Hood L, Readhead C. Identification of an embryonic isoform of myelin basic protein that is expressed widely in the mouse embryo. Proc Natl Acad Sci U S A 1993;90:10125–10129. [PubMed: 7694281]

Mazarati A, Lu X. Regulation of limbic status epilepticus by hippocampal galanin type 1 and type 2 receptors. Neuropeptides 2005;39:277–280. [PubMed: 15944022]

Mazarati AM, Hohmann JG, Bacon A, Liu H, Sankar R, Steiner RA, Wynick D, Wasterlain CG. Modulation of hippocampal excitability and seizures by galanin. J Neurosci 2000;20:6276–6281. [PubMed: 10934278]

Mazarati A, Lu X, Shinmei S, Badie-Mahdavi H, Bartfai T. Patterns of seizures, hippocampal injury and neurogenesis in three models of status epilepticus in galanin receptor type 1 (GALR1) knockout mice. Neuroscience 2004;128:431–441. [PubMed: 15350653]

Mazarati A, Lundström O, Sollenberg U, Shin D, Langel Ü, Sankar R. Regulation of kindling epileptogenesis by hippocampal galanin type 1 and type 2 receptors: the effects of subtype-selective agonists and the role of G-protein-mediated signaling. J Pharm Exp Ther 2006;318:700–708.

McColl CD, Jacoby AS, Shine J, Iismaa TP, Bekkers JM. Galanin receptor-1 knockout mice exhibit spontaneous epilepsy, abnormal EEGs and altered inhibition in the hippocampus. Neuropharmacology 2006;50:209–218. [PubMed: 16243364]

McKhann GM, Wenzel HJ, Robbins CA, Sosunov AA, Schwartzkroin PA. Mouse strain differences in kainic acid sensitivity, seizure behavior, mortality, and hippocampal pathology. Neuroscience 2003;122:551–561. [PubMed: 14614919]

McLin JP, Steward O. Comparison of seizure phenotype and neurodegeneration induced by systemic kainic acid in inbred, outbred, and hybrid mouse strains. Eur J Neurosci 2006;24:2191–2202. [PubMed: 17074044]

Minakuchi M, Kakazu N, Gorrin-Rivas MJ, Abe T, Copeland TD, Ueda K, Adachi Y. Identification and characterization of SEB, a novel protein that binds to the acute undifferentiated leukemia-associated protein SET. Eur J Biochem 2001;268:1340–1351. [PubMed: 11231286]

Nadler JV, Cuthbertson GJ. Kainic acid neurotoxicity toward hippocampal formation: dependence on specific excitatory pathways. Brain Res 1980;195:47–56. [PubMed: 6249441]

Nadler JV, Evenson DA. Use of excitatory amino acids to make axon-sparing lesions of hypothalamus. Methods Enzymol 1983;103:393–400. [PubMed: 6199648]

Nadler JV, Perry BW, Gentry C, Cotman CW. Degeneration of hippocampal CA3 pyramidal cells induced by intraventricular kainic acid. J Comp Neurol 1980;192:333–359. [PubMed: 7400401]

Notredame C, Higgins DG, Heringa J. T-Coffee: a novel method for fast and accurate multiple sequence alignment. J Mol Biol 2000;302:205–217. [PubMed: 10964570]

Noveroske JK, Hardy R, Dapper JD, Vogel H, Justice MJ. A new ENU-induced allele of mouse quaking causes severe CNS dysmyelination. Mamm Genome 2005;16:672–682. [PubMed: 16245024]

Ohgane J, Wakayama T, Senda S, Yamazaki Y, Inoue K, Ogura A, Marh J, Tanaka S, Yanagimachi R, Shiota K. The *Sall3* locus is an epigenetic hotspot of aberrant DNA methylation associated with placentomegaly of cloned mice. Genes Cells 2004;9:253–260. [PubMed: 15005712]

Parrish M, Ott T, Lance-Jones C, Schuetz G, Schwaeger-Nickolenko A, Monaghan AP. Loss of the Sall3 gene leads to palate deficiency, abnormalities in cranial nerves, and perinatal lethality. Mol Cell Biol 2004;24:7102–7112. [PubMed: 15282310]

Racine RJ. Modification of seizure activity by electrical stimulation. II. Motor seizure. Electroencephalogr Clin Neurophysiol 1972;32:281–294. [PubMed: 4110397]

Rozen S, Skaletsky H. Primer3 on the WWW for general users and for biologist programmers. Methods Mol Biol 2000;132:365–386. [PubMed: 10547847]

Sato K, Suematsu A, Nakashima T, Takemoto-Kumura S, Aoki K, Morishita Y, Asahara H, Ohya K, Yamaguchi A, Takai T, Kodama T, Chatila TA, Bito H, Takayanagi H. Regulation of osteoclast differentiation and function by the CaMK-CREB pathway. Nat Med 2007;12:1410–1416. [PubMed: 17128269]

Schauwecker PE. Genetic basis of kainate-induced excitotoxicity in mice: phenotypic modulation of seizure-induced cell death. Epilepsy Res 2003;55:201–210. [PubMed: 12972174]

Schauwecker PE, Steward O. Genetic determinants of susceptibility to excitotoxic cell death: implications for gene targeting approaches. Proc Natl Acad Sci U S A 1997;94:4103–4108. [PubMed: 9108112]

Schauwecker PE, Ramirez JJ, Steward O. Genetic dissection of the signals that induce synaptic reorganization. Exp Neurol 2000;161:139–152. [PubMed: 10683280]

Schauwecker PE, Williams RW, Santos JB. Genetic control of sensitivity to hippocampal cell death induced by kainic acid: a quantitative trait loci analysis. J Comp Neurol 2004;477:96–107. [PubMed: 15281082]

Schmued LC, Hopkins KJ. Fluoro-Jade B: a high affinity fluorescent marker for the localization of neuronal degeneration. Brain Res 2000;874:123–130. [PubMed: 10960596]

Shuttleworth CW, Connor JA. Strain-dependent differences in calcium signaling predict excitotoxicity in murine hippocampal neurons. J Neurosci 2001;21:4225–4236. [PubMed: 11404408]

Sidman, RL.; Angevine, JB.; Taber Pierce, E. Atlas of the Mouse Brain and Spinal Cord. Harvard University Press; Cambridge, MA: 1971.

Sousa N, Madeira MD, Paula-Barbosa MM. Effects of corticosterone treatment and rehabilitation on the hippocampal formation of neonatal and adult rats. An unbiased stereological study. Brain Res 1998;794:199–210. [PubMed: 9622630]

Sperk G, Lassmann H, Baran H, Kish SJ, Seitelberger F, Hornykiewicz O. Neurochemical and histopathological changes. Neuroscience 1983;10:1301–1315. [PubMed: 6141539]

Varon R, Gooding R, Steglich C, et al. Partial deficiency of the C-terminal-domain phosphatase of RNA polymerase II is associated with congenital cataracts facial dysmorphism neuropathy syndrome. Nat Genet 2003;35:185–189. [PubMed: 14517542]

West MJ, Slomianka L, Gundersen HJ. Unbiased stereological estimation of the total number of neurons in the subdivisions of the rat hippocampus using the optical fractionator. Anat Rec 1991;231:482–497. [PubMed: 1793176]

Yoshimura T, Arimura N, Kaibuchi K. Signaling networks in neuronal polarization. J Neurosci 2006;26:10626–10630. [PubMed: 17050700]

Zhao Q, Shao J, Chen W, Li YP. Osteoclast differentiation and gene regulation. Front Biosci 2007;12:2519–2529. [PubMed: 17127260]

Zini S, Roisin MP, Armengaud C, Ben-Ari Y. Effect of potassium channel modulators on the release of glutamate induced by ischaemic-like conditions in rat hippocampal slices. Neurosci Lett 1993a; 153:202–205. [PubMed: 8100991]

Zini S, Roisin MP, Langel U, Bartfai T, Ben-Ari Y. Galanin reduces release of endogenous excitatory amino acids in the rat hippocampus. Eur J Pharmacol 1993b;245:1–7. [PubMed: 7682961]

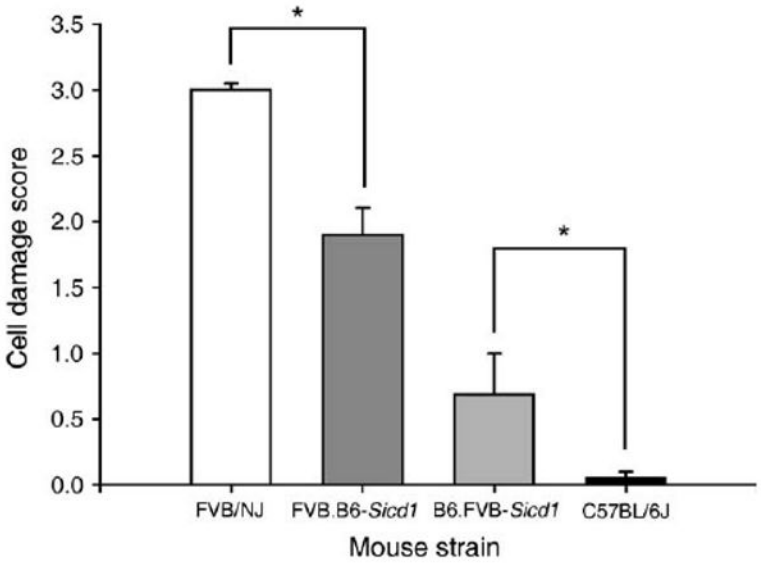

Figure 1. Confirmation that the FVB.B6-*Sicd1* and B6.FVB-*Sicd1* congenic strains capture a gene (s) that influences susceptibility to seizure-induced cell death

Data represent neuronal damage scores (in arbitrary units, mean ± SEM) for FVB.B6-*Sicd1* congenic, B6.FVB-*Sicd1* congenic, FVB/NJ and C57BL/6J strains. **P* < 0.05.

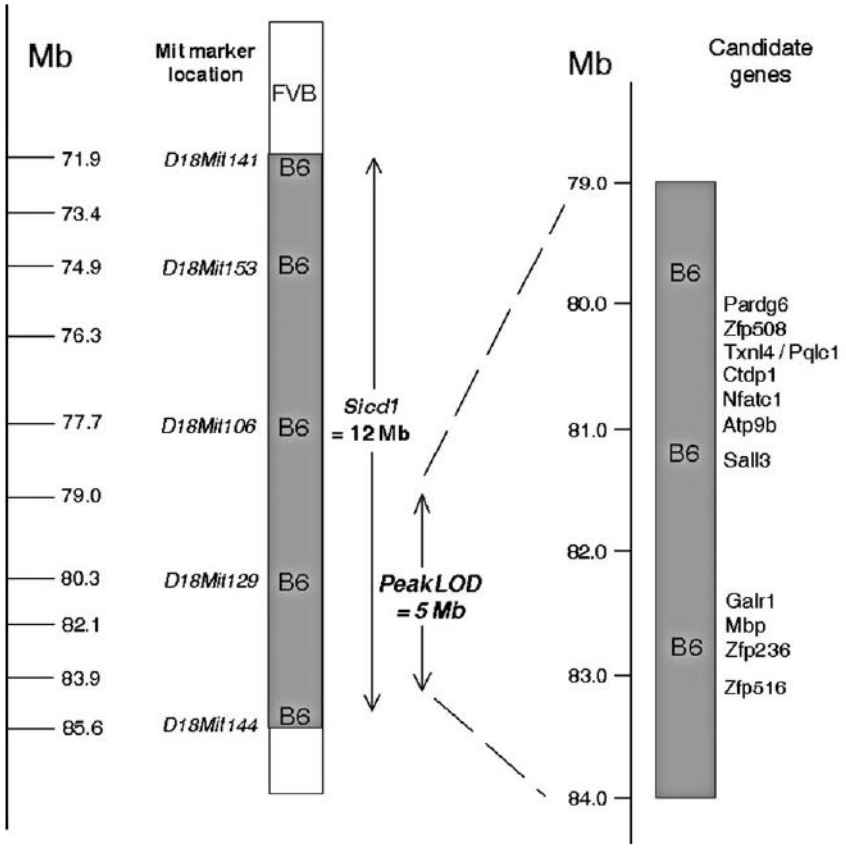

Figure 2. The position of the FVB.B6-*Sicd1* congenic segment responsible for reduced susceptibility to seizure-induced cell death and the 5-Mb peak LOD

The chromosome 18 region containing the *Sicd1* QTL is a 12-Mb interval between D18Mit141 and D18Mit144. The peak LOD region (79–84 Mb) contains an estimated 12 known candidate genes that show human homology. Map distance is illustrated in megabase and all distances are from http://www.ensembl.org.

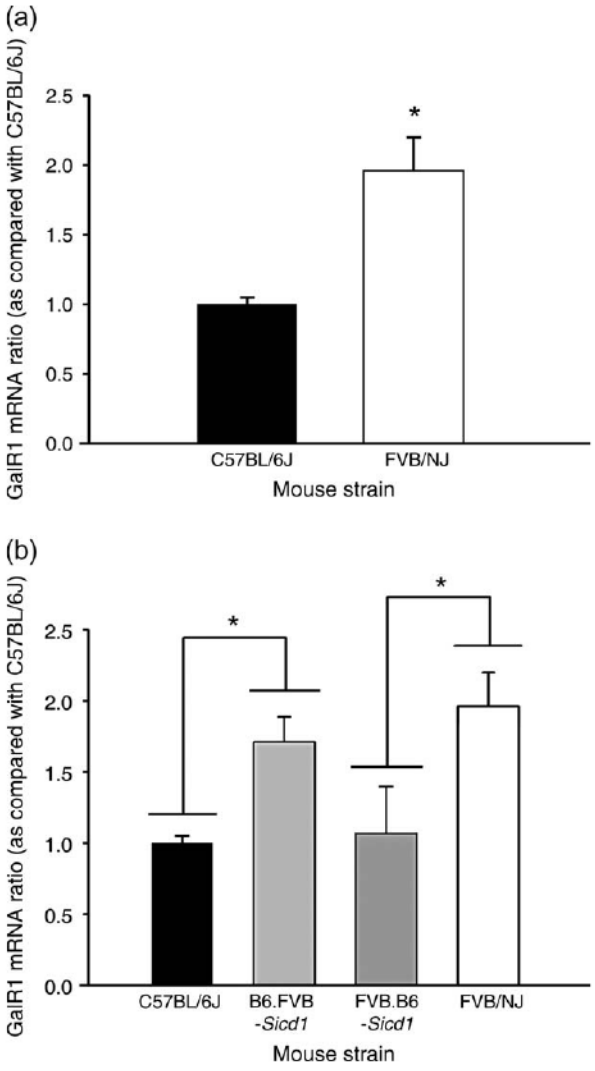

Figure 3. Basal hippocampal *Galr1* expression levels are differentially expressed in congenic and background strains

(a) Expression pattern of *Galr1* in parental strain tissue implicated in regulation of seizure-induced cell death. Quantitative real-time PCR expression of *Galr1* in hippocampus of the cell death-resistant B6 strain as compared with the cell death-susceptible FVB strain. Expression levels were standardized relative to β-actin transcript levels using the standard curve method. Values are provided as mean ± SEM from 6 to 11 mice per strain analyzed in triplicate. (b) Expression pattern of *Galr1* in congenic strain tissue. Quantitative real-time PCR expression of *Galr1* mRNA in hippocampus of wild-type (wt) B6, homozygous (HOMO) B6.FVB-*Sicd1* congenic, homozygous (HOMO) FVB.B6-*Sicd1* congenic, homozygous (HOMO) B6.FVB-*Sicd1* congenic and wild-type (wt) FVB mice. Data are expressed as mean ± SEM from 6 to 11 mice per strain analyzed in triplicate. Ratios show the change in mRNA expression compared with C57BL/6J mice (no change = ratio of 1). *$P < 0.05$.

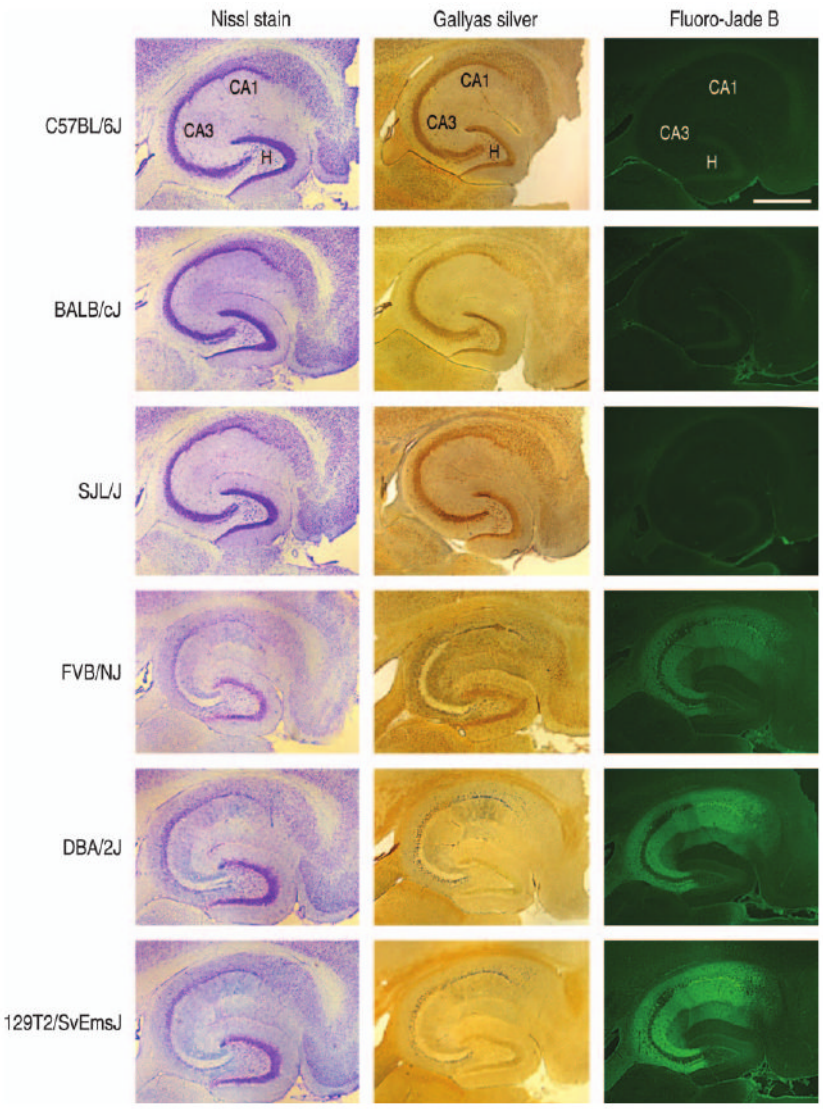

Figure 4. Neuronal cell loss and degeneration after kainate in six inbred strains of mice, as depicted by cresyl violet (Nissl stain), the degenerative Gallyas silver stain and Fluoro-Jade staining

Note the destruction of neurons in the CA3 and CA1 subfields and within the dentate hilus 7 days after kainate administration in the FVB/NJ, DBA/2J and 129T2/SvEmsJ strains. Cell loss was not observed after kainate administration in C57BL/6J, BALB/cJ or SJL/J strains of mice. CA3, CA3 pyramidal cell layer; CA1, CA1 pyramidal cell layer and H, hilus. Scale bar = 750 μm.

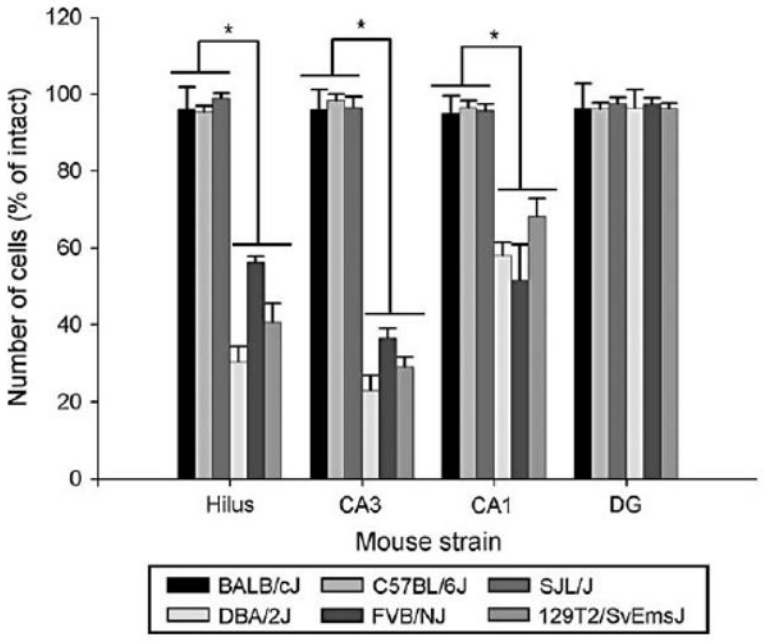

Figure 5. Quantification of strain differences in seizure-induced cell death in hippocampal subfields in resistant (BALB/cJ, C57BL/6J and SJL/J) and susceptible (DBA/2J, FVB/NJ and 129T2/SvEmsJ) strains of mice

Viable surviving neuronal profiles were estimated by cresyl violet staining. Bars denote the percentage of surviving neuronal profiles (as compared with saline-injected control mice of each representative strain) in each hippocampal region. Comparison of neuron profile counts between 'susceptible' and 'resistant' mouse strains showed statistically significant differences. Data represent the mean ± SEM of eight mice per strain. *$P < 0.05$.

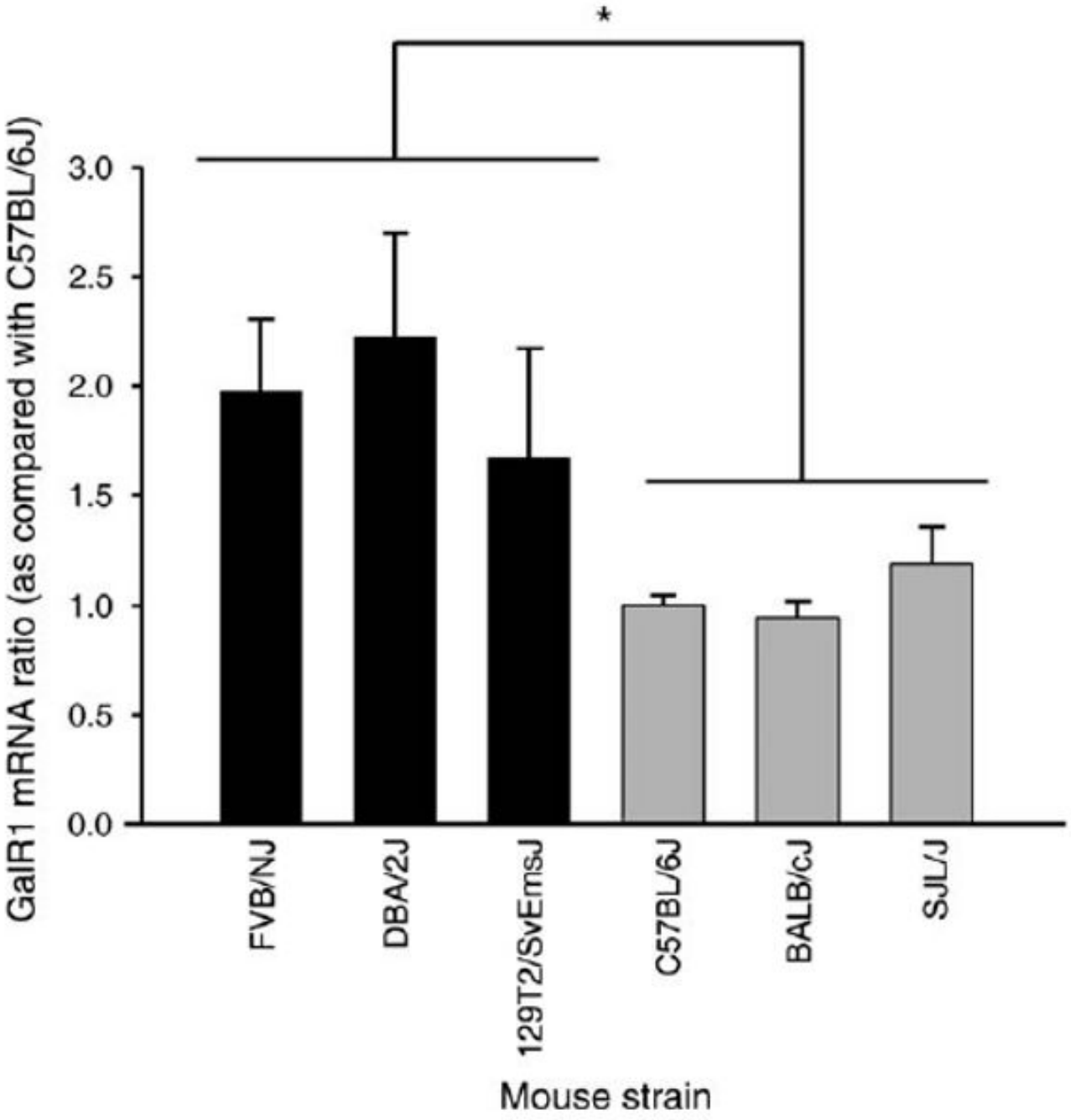

Figure 6. Expression of the *Galr1* gene in hippocampi of six inbred strains of mice

Relative basal *Galr1* transcript levels were measured in hippocampi of six commonly used inbred strains that differ with regard to susceptibility to KA-induced excitotoxic cell death. Black bars indicate susceptible (FVB/NJ, DBA/2J and 129T2/SvEmsJ) strains and gray bars indicate resistant (C57BL/6J, BALB/cJ and SJL/J) strains. Basal hippocampal *Galr1* transcript levels were significantly lower (30–60%) in cell death-resistant strains as compared with cell death-susceptible strains. Data are presented as mean ± SEM ($n = 8$ per strain). Ratios show the change in mRNA expression compared with C57BL/6J mice (no change = ratio of 1). *$P < 0.05$.

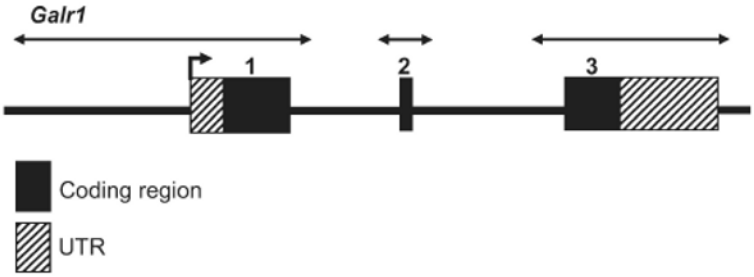

Figure 7. Genomic map of the murine *Galr1* gene. Exons are shown as boxes separated by introns depicted as lines

The UTRs are depicted as hatched boxes. Double-pointed arrows indicate the sequenced region. Gaps in introns 1 and 2 refer to sequencing gaps. No sequencing differences between the FVB and the B6 genomes were found.

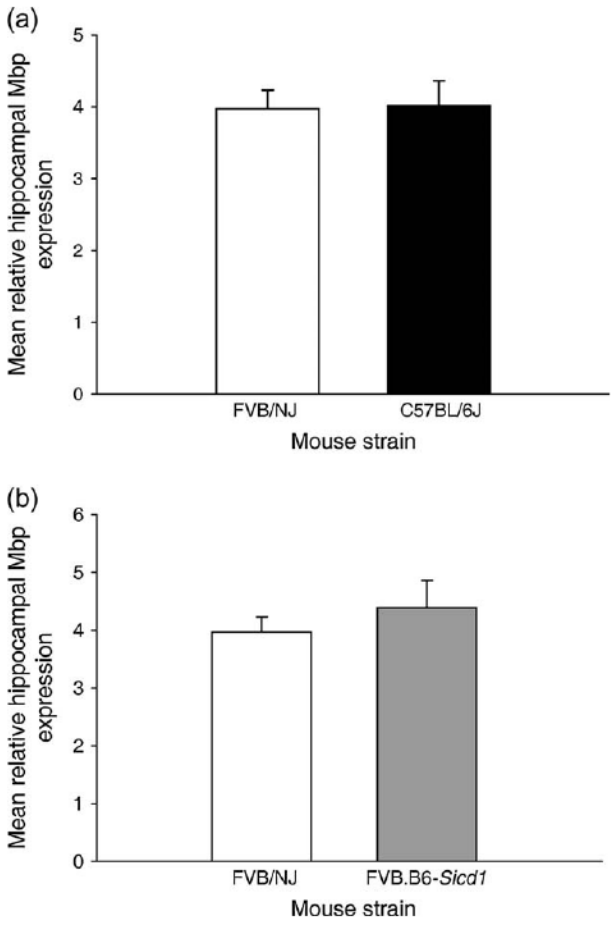

Figure 8. Basal hippocampal *Mbp* expression levels in the parental inbred mouse strains, B6 and FVB and in congenic FVB.B6-*Sicd1* mice

(a) Quantitative real-time PCR expression of *Mbp* in hippocampus of the cell death-resistant B6 (C57BL/6J) strain and the cell death-susceptible FVB strain. Expression levels were standardized relative to β-actin transcript levels using the standard curve method. Values are provided as mean ± SEM from 11 to 18 mice per strain analyzed in triplicate. (b) Expression pattern of *Mbp* in congenic strain tissue. Quantitative real-time PCR expression of *Mbp* mRNA in hippocampus of wild-type (wt) FVB and homozygous (HOMO) FVB.B6-*Sicd1* congenic mice. Data are expressed as mean ± SEM from 11 to 18 mice per strain analyzed in triplicate. $*P < 0.05$.

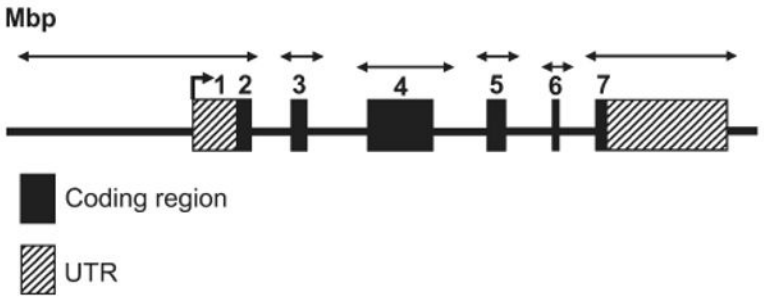

Figure 9. Genomic map of the murine *Mbp* gene. Exons are shown as boxes separated by introns depicted as lines

The UTRs are depicted as hatched boxes. Double-pointed arrows indicate the sequenced regions. Gaps in introns 2–6 refer to sequencing gaps. No sequencing differences between the FVB and the B6 genomes were detected.

Figure 10. Comparison of the nucleotide sequences of C57BL/6J and FVB/NJ murine *Galr1* cDNA

Nucleotide sequences of the B6 and FVB *Galr1* cDNA were aligned using the T-Coffee program (Notredame *et al.* 2000). Conserved nucleotide identities between the two strains are indicated by a '*'. The PolyA region is in bold. Note that no *Galr1* cDNA sequence variants were identified between these two strains.

Table 1

Quantitative real-time PCR primers of *Galr1, Mbp* and *β-actin*

Name	Region	Sequence	Size in bp
Galr1	Galr1-F	CTTACTGCTCATCTGCTTTTGCTAT	100
	Galr1-R	AGTCTTTTTCTTGGATGCTTCAGAC	
Mbp	Mbp-F	CCACTCTTGAACACCCCATT	100
	Mbp-R	TCCTCGGTGAATCTCTCCAT	
β-actin	β-actin-F	TGACCCAGATCATGTTTGAGA	357
	β-actin-R	TCTCCAGGGAGGAAGAGGAT	

Table 2

Sequencing primers of Galr1 genomic DNA

Genomic DNA region	Name	Sequence	Size in bp
Promoter	g-p-1F	GGATCAGAAGGGCCAAAAG	739
	g-p-1R	TGATCCTTGCCTCTTCCTTG	
Promoter	g-p-2F	CAGAGGGAGCAGCTTGTAGG	697
	g-p-2R	GAGCCTTGGTTGAGGAAATG	
Promoter	g-p-3F	CTGCTTACTGGCTTGCTTCC	690
	g-p-3R	TGTGACTGCGTGTGTGTGAT	
Promoter	g-p-4F	AAGTGCCAGCGTACACACAC	695
	g-p-4R	TAACACACTGCCAGGGACAC	
Promoter	g-p-4-1F	CAGGGCATAAAAGCACTTCC	806
	g-p-4-1R	TAACACACTGCCAGGGACAC	
Promoter	g-p-5F	TAAGGATGCTCTCCGATGCT	621
	g-p-5R	TCCATCATTTCCACCAGACA	
Promoter	g-p-6F	GGCCTTTCACCACAGTCAA	631
	g-p-6R	CTGAGCTTCCCGCACTAAGA	
Promoter	g-p-7F	CAGAATCTCTGCTGGCCACT	603
	g-p-7R	GGAAAACTGGCTCTGGAGGT	
5′-UTR	g-5′utr-F	GGATGCATTTGAATATTCACAGTC	746
	g-5′utr-R	CATTCCCTTCACTGAGGTTCA	
EX 1	g-ex1-F	GAAAGGCTTAGCTCGGGACT	677
	g-ex1-R	GTAGCGATCCACAGACATCG	
EX 1-1	g-ex1-1F	GGTGCTCTTCTGCATCCCTTT	553
	g-ex1-1R	CGGAGAAAGCAAGCTGAGAC	
EX 2	g-ex2-F	TTGGAGCCTGGTTTATGCT	614
	g-ex2-R	TGACAGTTTCGAATCATCCCTA	
EX 3	g-ex3-F	CAGCGCTGTATTCTCCTGAT	683
	g-ex3-R	ATCAAAACATTTGCAGAGTGCT	
3′ -UTR-1	g-3′utr-1F	GGCAGCTTATTCTCCACAGC	444
	g-3′utr-1R	CTCACATCCCCAGACAGACC	
3′ -UTR-2	g-3′utr-2F	TGTGCTTTGAAATACAACGTGG	471
	g-3′utr-2R	TTTGTAAGTCACATGGTGATGG	

Table 3

Sequencing primers of the *Mbp* genomic DNA

Genomic DNA region	Name	Sequence	Size in bp
Promoter	m-p-1F	GAGTCCGCCTGTACTCTGCT	732
	m-p-1R	TACTATGTTCCGGGGTCGTG	
Promoter	m-p-2F	TTTGCCAATGGTCTAACAGG	782
	m-p-2R	TGTAGACGCTGCTTCTTTGG	
Promoter	m-p-3F	TCAGGCTCTCAAGTTTGCAC	770
	m-p-3R	TTCAGGTCAGCAACCAGATG	
Promoter	m-p-4F	TTGTTCGCATCAGGTTTTCC	740
	m-p-4R	TCAACAGCTCACACCTCAGC	
Promoter	m-p-5F	TGAAAGGAAAACCGGAAAAC	497
	m-p-5R	TCAACAGCTCACACCTCAGC	
Promoter	m-p-6F	GGCCTACTGCAGGAAACAAA	553
	m-p-6R	GGGCTGGTCTGTTGTCTCAC	
Promoter	m-p-7F	ACCAACCCCTGTAGAAAGCA	445
	m-p-7R	TTTGCCGTTTTCTTGAGGTC	
Promoter	m-p-8F	CTACCCCACGGTCTGTCTG	475
	m-p-8R	TGCTTTCTACAGGGGTTGGT	
Promoter	m-p-9F	GAGTGCTTCCTGTTCCTCCA	792
	m-p-9R	TTCCTGTGTGACTTGGCACT	
Promoter	m-p-10F	GTGGCCCTTCTTTGGTACTG	791
	m-p-10R	GGTTGTTGCGGTCTGTGTAG	
5′-UTR	m-5′utr-F	GAAGCAATAAAGTCCAGAGAGCA	481
	m-5′utr-R	CGCCTCTCAAGGAGTCAGAT	
EX 1	m-ex1-F	CTCGATCTTTCCCTGAGAGC	410
	m-ex1-R	GATGGATGGACCCACTGAGA	
EX 2	m-ex2-F	CAGCCTGTCTTGTCTGCTTG	498
	m-ex2-R	TTGTGTTCACATCCGGAAAC	
EX 3	m-ex3-F	TCAAGACCCCAGGAAGAAAG	606
	m-ex3-R	GTTGCTCTGCGATGGTGACT	
EX 4	m-ex4-F	ACCTGGCAAACTGGTGGTTA	455
	m-ex4-R	TCCTTTAGGACCTGGGATGA	
EX 5	m-ex5-F	TCAGTAGATGTGCCATTTCCA	383
	m-ex5-R	GACCTGCTGCATCTCTGTCC	
EX 6	m-ex6-F	TTGGACAACCACAGAACCAG	658
	m-ex6-R	CAGCCTGTGCTCACATACCA	
3′-UTR-1	m-3′utr-1F	TGCGGATAGACAGGCACAC	711
	m-3′utr-1R	ACTGGGGTTCTCAGCTCCTC	
3′-UTR-2	m-3′utr-2F	ATAACCATTCCCTGCCT	617
	m-3′utr-2R	ACGAGGCTGTGCTTCACTC	

Table 4

Reverse transcriptase primer pair of full-length hippocampal Galr1 cDNA

Name	Region	Sequence	Size (bp)
Galr1	galr1-F	CCTAGACCCGTACCTCTGTGT	1904
	galr1-R	GGTCTCACATCCCCAGACA	

Table 5

Classification of seizure parameters in inbred strains of mice after systemic administration of KA

	Seizure parameters, percentage of mice				
Mouse strain	**Staring**	**Rigid posture**	**Repetitive movements**	**Rearing and falling**	**Duration of seizures (h)**
BALB/cJ (*n* = 11)	100	100	100	100	1.27
C57BL/6J (*n* = 10)	100	100	100	97.5	1.35
DBA/2J (*n* = 10)	100	100	100	100	2.10*
FVB/NJ (*n* = 13)	100	100	92.3	98.3	1.42
129T2/SvEmsJ (*n* = 10)	100	100	100	100	1.40
SJL/J (*n* = 10)	100	100	100	97.3	2.08*

While KA induced a similar level of stage irrespective of mouse strain ($F = 0.719$; $P = 0.621$), a significant strain-dependent difference in the duration of severe seizures was observed (*$P < 0.05$).